Carbohydrate Polymers 117 (2015) 887–894

Contents lists available at ScienceDirect

Carbohydrate Polymers

journal homepage: www.elsevier.com/locate/carbpol

Contact time- and pH-dependent adhesion and cohesion of low molecular weight chitosan coated surfaces

Chanoong Lim[a,1], Dong Woog Lee[b,1], Jacob N. Israelachvili[a], YongSeok Jho[c,d], Dong Soo Hwang[a,e,f,*]

[a] School of Interdisciplinary Bioscience and Bioengineering, Pohang University of Science and Technology (POSTECH), Pohang 790-784, South Korea
[b] Department of Chemical Engineering, University of California at Santa Barbara, CA 93106, USA
[c] Asia Pacific Center for Theoretical Physics, Pohang, Gyeongbuk 790-784, South Korea
[d] Department of Physics, Pohang University of Science and Technology, Pohang, Gyeongbuk 790-784, South Korea
[e] School of Environmental Science and Engineering, Pohang University of Science and Technology (POSTECH), Pohang 790-784, South Korea
[f] Integrative Biosciences and Biotechnology, Pohang University of Science and Technology (POSTECH), Pohang 790-784, South Korea

ARTICLE INFO

Article history:
Received 12 July 2014
Received in revised form 8 October 2014
Accepted 9 October 2014
Available online 5 November 2014

Keywords:
Biomolecule
Low molecular weight chitosan
Surface forces apparatus
Adhesion
Cohesion
Solubility

ABSTRACT

Low molecular weight chitosan (LMW chitosan, ~5 kDa) potentially has many desirable biomedical applications such as anti-microbial, anti-tumor, and anti-diabetes. Unlike high molecular weight chitosan, LMW chitosan is easily dissolvable in aqueous solutions even at neutral and basic pH, but its dissolution mechanism is not well understood. Here, we measured adhesion and cohesion of molecularly thin LMW chitosan films in aqueous solutions in different buffer pHs (from 3.0 to 8.5) using a surface forces apparatus (SFA). Interestingly, significantly lower adhesion force was measured for LMW chitosan films compared to the high molecular weight chitosan (~150 kDa) films. Not only the strength of adhesion is lower, but also the critical contact time where adhesion starts to increase with contact time is longer. The results from both the SFA and atomic force microscopy (AFM) indicate that, in physiological and basic conditions, the low cohesion of LMW chitosan due to the stiffness of the chain which cause strong electrostatic correlation energy penalty when they are aggregated. Here, we propose the reduction in cohesion for shorter chitosan (LMW chitosan) as an explanation of its high solubility of LMW chitosan in physiological pHs.

1. Introduction

Chitin and chitosan are random copolymers composed of D-glucosamine and *N*-acetyl-D-glucosamine units connected by β-1,4 linkages. The mole ratio of D-glucosamine and *N*-acetyl-D-glucosamine in the copolymers determines the two terms, chitin and chitosan. Conventionally, the copolymer with higher mole fraction of D-glucosamine unit is defined as chitosan, and the opposite case is called chitin. Mole fraction of D-glucosamine unit in chitin and chitosan is defined as degree of acetylation (DA) on D-glucosamine units. Generally, chitosan is obtained by deacetylation and hydrolysis of chitin, which is the second most abundant biomolecules in the nature (Chang, Tsai, Lee, & Fu, 1997; Ifuku et al., 2009; Mima, Miya, Iwamoto, & Yoshikawa, 1983). Wide ranges of molecular weight of chitosan (from 1 kDa to 200 kDa) are produced from chitin, and their physical and biological properties of chitosan differ as their molecular weight. To date, diverse forms of chitosan have been used in many applications including healthcare, agriculture, environmental engineering, medical engineering and cosmetics (Kumar, Muzzarelli, Muzzarelli, Sashiwa, & Domb, 2004; Kurita, 1998, 2006; Rabea, Badawy, Stevens, Smagghe, & Steurbaut, 2003; Ravi Kumar, 2000).

Unlike the chitosan, low molecular weight chitosan (LMW chitosan, ≤10 kDa) is easily dissolvable even in buffer solutions at physiological pHs because of its shorter chain length. The good solubility and low viscosity of LMW chitosan at physiological pHs have attracted public attention to utilize LMW chitosan in biomedical applications. Indeed, a number of desirable biomedical applications of LMW chitosan have been suggested, such as blood thinning, cholesterol-lowering, anti-oxidant, and anti-microbial properties (Busilacchi, Gigante, Mattioli-Belmonte, Manzotti, & Muzzarelli,

* Corresponding author at: School of Interdisciplinary Bioscience and Bioengineering, Pohang University of Science and Technology (POSTECH), Pohang 790-784, South Korea. Tel.: +82 54 279 9505; fax: +82 54 279 9519.
E-mail address: dshwang@postech.ac.kr (D.S. Hwang).
[1] These authors equally contributed on this work.

http://dx.doi.org/10.1016/j.carbpol.2014.10.033
0144-8617/

2013; Felt, Buri, & Gurny, 1998; Hirano, Seino, Akiyama, & Nonaka, 1990; Muzzarelli, 2009). However, many previous studies on biomedical applications of LMW chitosan do not cover molecular mechanisms in detail (Muzzarelli, 2009). Therefore, investigating molecular interactions and solubility of LMW chitosan in aqueous buffers may help to unravel its mechanisms for the biomedical applications eventually leading to a better and broader use of LMW chitosan.

Surface forces apparatus (SFA) is one of the ideal biomechanical tools for measure molecular interactions of bioactive molecules in wet conditions (Israelachvili, 2011) with nano-Newton force sensitivity and angstrom distance resolution. It has been used not only to measure normal adhesion forces (Lee et al., 2014), but also lateral friction forces (Lee, Banquy, & Israelachvili, 2013). Recently, pH- and contact time-dependent interactions of chitosan (Mw ~ 150 kDa) were measured with an SFA (Lee, Lim, Israelachvili, & Hwang, 2013). Strong cohesion ($W_{co} \sim 8.5\ mJ/m^2$) between the two opposing chitosan films was measured in acidic pH, which is more than a half of the strongest, previous reported, mussel wet adhesion (Hwang, Zeng, Lu, Israelachvili, & Waite, 2012; Hwang et al., 2010). However, the interaction of LMW chitosan in aqueous solutions, and its relationship with higher solubility of LMW chitosan compared to that of high molecular weight chitosan have not been studied yet even though many desirable biomedical activities and potential for biomedical applications of LMW chitosan.

In this study, we measured cohesion and adhesion of molecularly thin LMW chitosan (Mw ~ 5 kDa) films using an SFA in buffers with different pHs (from 3.0 to 8.5, Fig. 1). This work not only provides fundamental understandings on the molecular mechanisms of LMW chitosan interactions in aqueous solutions at different buffer pHs.

2. Materials and methods

2.1. Sample preparation and characterization

Chitosan (LMW chitosan, Mw ~ 5 KDa) was purchased from Chitolife (Seoul, South Korea). The degree of acetylation (DA) of LMW chitosan (~11%) was determined by previously reported ^{1}H NMR base assay (de Alvarenga, Pereira de Oliveira, & Roberto Bellato, 2010; Hirai, Odani, & Nakajima, 1991). The polydispersity index of LMW chitosan measured by Dynamic light scattering was 0.3. LMW chitosan solution was prepared by dissolving LMW chitosan in 150 mM acetic acid buffer (pH 3.0), with final concentration of 50 μg/mL. Prepared LMW chitosan solution was used throughout the experiments for surface forces measurements and chemical analysis. Three buffers with different pHs were prepared: 150 mM acetic acid (pH 3.0), 150 mM sodium acetate buffer (pH 6.5), and 150 mM phosphate buffer (pH 8.5). All aqueous solutions were prepared in Milli-Q water (Millipore, Billeriaca, MA, USA) and filtered through 0.22 μm PTFE filters (Millipore, Billeriaca, MA, USA).

2.2. Surface preparation and LMW chitosan film deposition

Muscovite mica surfaces (Grade #1, S&J Trading, Floral Park, NY, USA) were freshly cleaved under a dust free laminar flow hood. 55 nm of silver layer was deposited using a Joule effect vapor deposition. Thin and back-silvered mica sheets was glued (silver side down) on cylindrical glass disks using an epoxy glue (EPON 1004 F®, Exxon Chemicals, Irving, TX, USA). LMW chitosan was deposited on the back silvered mica surfaces according to previous reported procedures (Lee, Lim, et al., 2013). Briefly, 1 ml of the prepared chitosan solution (50 μg/ml in 150 mM acetic acid, pH 3.0) is dropped onto the mica surface and incubated for 20 min in a water saturated chamber. Then the surface was rinsed thoroughly with the acidic buffer solution (150 mM acetic acid, pH 3.0) in order to remove unbound and weakly bound chitosan.

2.3. Interaction force measurements using an SFA

The adhesion and cohesion forces of LMW chitosan films were determined using a surface forces apparatus 2000 (Surforce LLC, Santa Barbara, CA, USA) in a configuration that was previously reported in literature (Lee, Lim, et al., 2013). Depending on the experiments, either two opposing LMW chitosan coated surfaces (symmetric) or one LMW chitosan coated surface and one mica surface (asymmetric) were transferred into the SFA chamber in cross-cylinder geometry which corresponds to a sphere of radius R (~2 cm) approaching a flat surface. A droplet (50 μl) of buffer (pH 3.0) was injected between the transferred surfaces. The SFA chamber was sealed and saturated with water vapor during the experiments. After mounting of the surfaces and injection of the buffer, the system was allowed to equilibrate for 1 h. All experiments were conducted at room temperature ($T = 23\ ^\circ C$).

The interaction forces F between the two opposing chitosan films in aqueous buffer were measured as a function of the absolute surface separation distance D between two surfaces. F was measured by the deflection of the double cantilever spring ($k = 3030\ N/m$) of the lower surface and D was determined using multiple beam interferometry (MBI) (Israelachvili, 1973; Israelachvili et al., 2010; Israelachvili & Tabor, 1972). During a typical SFA force measurements, the two opposing surfaces was brought toward each other by a motor driven micrometer to reach a "steric wall distance" (D_{sw}) and kept in contact for a desired time, followed by separation. In the repulsive regime of the force curve ($F/R > 0$), the interaction force F can be converted to the interaction energy W by using Derjaguin approximation ($W = F/2\pi R$) (Israelachvili, 2011; Johnson, Kendall, & Roberts, 1971). Adhesion force F_{ad} (for asymmetric mode) and cohesion force F_{co} (for symmetric mode) are measured during separation and the surfaces jump apart from adhesive contact when the tensile load exceeds F_{ad} or F_{co} (F_{ad}/R and F_{co}/R defined as -min [F/R] to achieve positive values). The adhesion energy per unit area W_{ad} can be calculated by Johnson–Kendal–Roberts theory (Israelachvili, 2011; Johnson et al., 1971), where $W_{ad} = 2F_{ad}/3\pi R$ for soft deformable surfaces.

The surfaces were approached at a constant speed of ~3 nm/s to contact (up to $F/R \sim 4\ mN/m$) and kept in contact for 5 s, 2 min, 10 min, and 1 h, followed by separation to investigate the effect of contact time on cohesion/adhesion forces of the LMW chitosan films. Force vs distance curves were measured at least 3 times at each condition to confirm their reproducibility. In addition to the force measurement under the pH 3.0 buffer, the measurements were repeated after replacing the buffer with an excess amount of 150 mM sodium acetate buffer solution (pH 6.5) and 150 mM phosphate buffer solution (pH 8.5) to study the effects of pH.

2.4. Surface topography study using atomic force microscopy (AFM)

A LMW chitosan film was adsorbed onto freshly cleave mica surface by placing a chitosan solution (10 μg/ml in 150 mM acetic acid, pH 3.0) for 20 min, and followed by a thorough rinsing with the buffer solution (150 mM acetic acid, pH 3.0) in order to remove unbound LMW chitosan. The LMW chitosan film on mica surface was incubated for 1 h under three different pHs (3.0, 6.5, 8.5). The surfaces were imaged using a Nanoscope III AFM (Veeco, Santa Barbara, CA, USA) using a silicon nitride probe (Olympus, Tokyo, Japan), with a spring constant of 0.35 N/m in wet conditions. Scannings

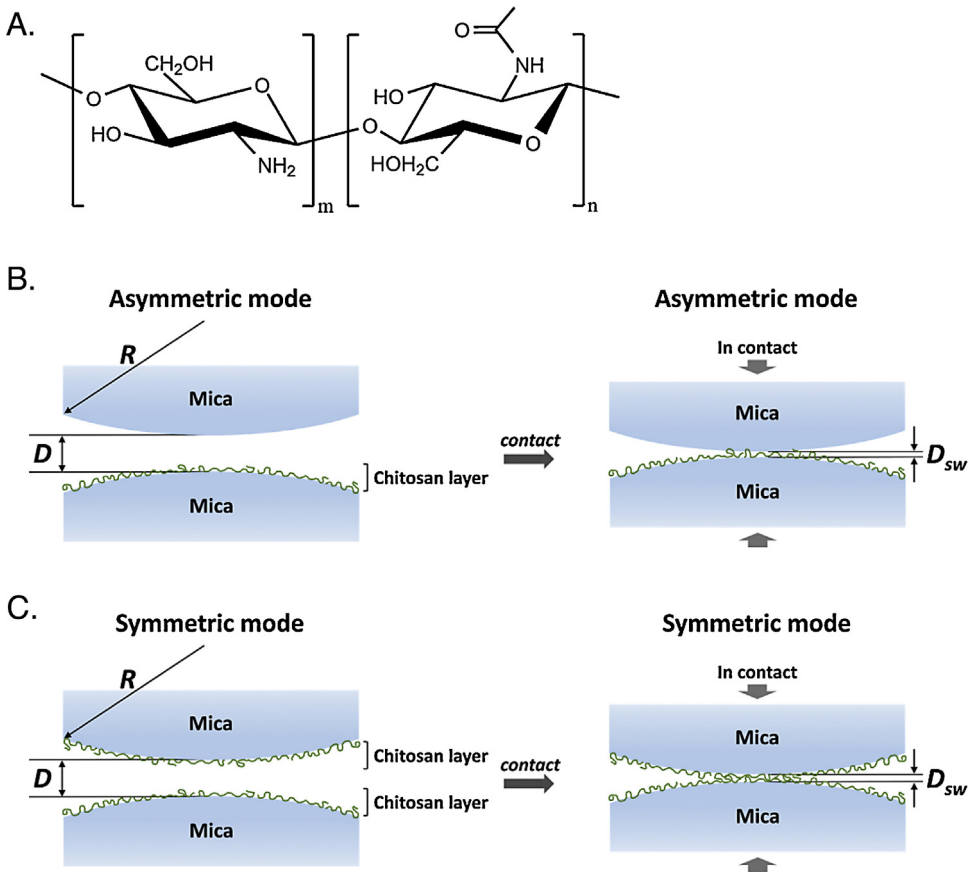

Fig. 1. (A) Chemical structures of chitosan molecule. Chitosan is copolymers of D-glucosamine (m) and N-acetyl-D-glucosamine (n) unit ($m > n$). (B) Schematic figures of separated mica surfaces with distance, D, in asymmetric mode (left), contacted mica surfaces mode with a steric wall distance (D_{sw}) in asymmetric mode (Right). (C) Schematic figures of separated mica surfaces in symmetric mode. R is the radius of the surfaces.

were performed in tapping mode at room temperature (~23 °C) in three different pHs (3.0, 6.5, 8.5).

3. Results and discussion

3.1. LMW chitosan coating on mica surface

The degree of acetylation (DA) determines physicochemical and biological properties of Chitosan (LMW chitosan, Mw ~ 5 kDa) (Cabrera, Boland, Cambier, Frettinger, & Van Cutsem, 2010; Freier, Koh, Kazazian, & Shoichet, 2005). Solubility of LMW chitosan in aqueous solutions, surface smoothness of the LMW chitosan film, and cell proliferation on the LMW chitosan film decrease, when the DA of LMW chitosan increases (Chatelet, Damour, & Domard, 2001). These phenomena suggest that the DA of LMW chitosan is one of the key factors for interactions of LMW chitosan. Therefore, prior to measuring interactions of LMW chitosan, the DA of LMW chitosan was determined by ^{1}NMR. The DA of LMW chitosan used in this study was ~11%, which is slightly lower than that of previously studied chitosan (DA ~ 19%, Mw ~ 150 kDa) using an SFA (Lee, Lim, et al., 2013).

To monitor surface topographical changes with pH, we prepared LMW chitosan adsorbed mica surfaces (Fig. 2) following the procedure in materials and methods. Atomic force microscopy (AFM) images of LMW chitosan coated mica in wet conditions were generated after incubation with the buffer solutions at three different pHs (3.0, 6.5, and 8.5). AFM images revealed that a smooth chitosan film on mica was roughened by pH elevation. The root-mean-square (RMS) roughness determined by AFM for LMW chitosan coated surfaces at pH 3.0, 6.5, and 8.5 were ~0.142 nm, ~0.204 nm, and ~0.236 nm, respectively (Fig. 2).

3.2. Interactions of LMW chitosan

After LMW chitosan-adsorbed surface preparation, interaction forces between one LMW chitosan film and bare mica (asymmetric mode, adhesion) or two opposing LMW chitosan films (symmetric mode, cohesion) were measured using an SFA in the aqueous buffer solutions at three different pHs (3.0, 6.5, and 8.5, Fig. 1). Since previous reported pKa value of LMW chitosan is about 6.5, the level of protonation in amine group of D-glucosamine units varies with pH: glucosamine units in LMW chitosan film on mica would be fully protonated at pH 3.0, half of the glucosamine units would be protonated at pH 6.5, and most of the D-glucosamine units would be deprotonated at pH 8.5.

3.2.1. Adhesion of LMW chitosan to mica (asymmetric mode)

For force measurement between the LMW chitosan film and negatively charged bare mica, two surfaces were immersed in 150 mM acetic acid buffer at pH 3.0 and brought to together to reach a steric wall, D_{sw}. The D_{sw} is defined as the two bare mica surfaces separation distance (D) when the distance (D) does not apparently change with the increase in the normal compressive load. Generally, the D_{sw} provides thickness of confined film trapped between two opposing mica surfaces in the SFA experiment. Here, D at $F/R = 4$ mN/m was designated as D_{sw}. An adhesion force (F_{ad}/R) ~ 12 mN/m and D_{sw} ~3 nm were measured after the contact time, t_{ct}, of 5 s. When the t_{ct} was increased to 1 h, the adhesion force monotonically increased up to F_{ad}/R ~ 17 mN/m

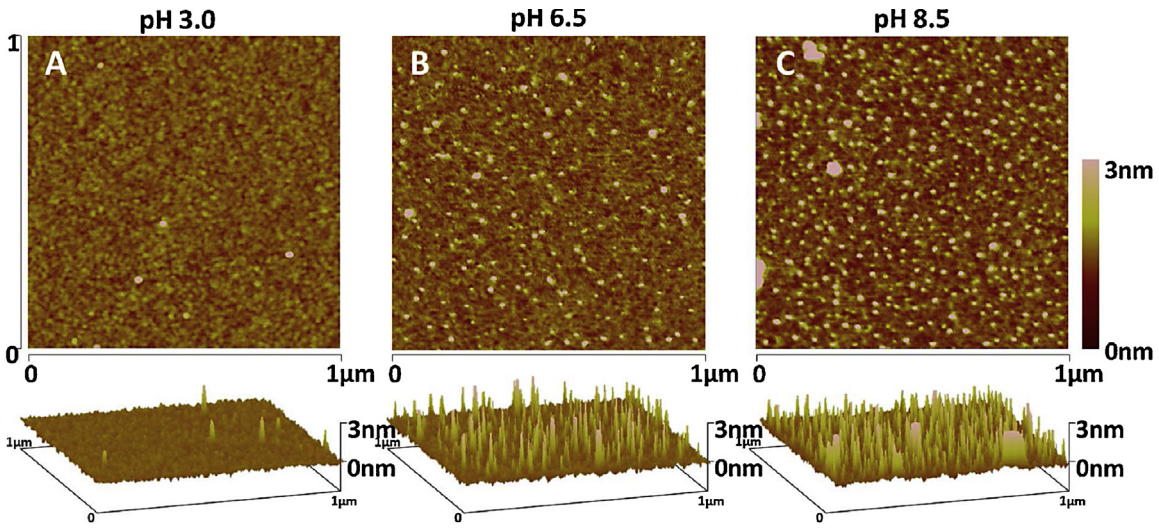

Fig. 2. AFM tapping mode images of low molecular weight chitosan (LMW chitosan) films deposited at pH 3.0 on freshly cleaved muscovite mica and incubated for 1 h (A) at pH 3.0, (B) at pH 6.5, and (C) at pH 8.5.

(Figs. 3A and 5) and D_{sw} decreased down to ~0.8 nm (Fig. 3A) which is slightly thinner than that of chitosan (~150 kDa) reported in previous studies (Lee, Lim, et al., 2013). In addition, hysteresis was observed between approach (which is purely repulsive) and separation force curves (adhesive) even after very short contact time (t_{ct} < 5 s). These results indicate that a rearrangement and/or possible structural change – possibly from the relaxed two-fold helix to the extended two-fold helix (Lertworasirikul, Tsue, Noguchi, Okuyama, & Ogawa, 2003; Okuyama, Noguchi, Miyazawa, Yui, & Ogawa, 1997) – of LMW chitosan molecules have occurred due to the external force in a confined space which caused the LMW chitosan layer to be more compact and adhesive to the opposing mica substrate. The adhesions of LMW chitosan to mica were ~40% less than those of previous studied higher molecular weight chitosan (~150 kDa) to mica (Lee, Lim, et al., 2013). Electrostatic interaction may account for the initial adhesion force (when $t_{ct} < t_{crit}$) between positively charged chitosan film and negatively charged mica. Poly-L-lysine, which has similar positive charged density and molecular weight (Mw ~ 4 kDa) as LMW chitosan, showed similar initial attractive force to mica surface ($F_{ad}/R \sim 17$ mN/m) in the previous SFA experiment (Afshar-Rad, Bailey, Luckham, Macnaughtan, & Chapman, 1987). The increase in adhesion force with contact time (when $t_{ct} > t_{crit}$) is attributed to the hydrogen bonding between LMW chitosan film and mica which is also related to the mobility of the hydrogen donor/acceptor residues.

To examine effect of positive charges in chitosan, additional force measurements between the LMW chitosan film and mica were performed at pH 6.5 (around pKa of LMW chitosan, Fig. 3B) and pH 8.5 (Fig. 3C). The adhesion of LMW chitosan film to mica decreased monotonically with decreasing protonation of the amines in LMW chitosan. Adhesion of LMW chitosan to mica at pH 6.5 was reduced to approximately 50% of its value at pH 3.0, which is roughly corresponding to 50% deprotonation of LMW chitosan. Moreover, the adhesion of LMW chitosan to mica at pH 8.5 was significantly reduced. LMW chitosan and negatively charged mica could not interact electrostatically anymore as most amine groups in LMW chitosan are deprotonated at pH 8.5. A weak adhesion (~3 mN/m) with 1 h contact between the LMW chitosan film and mica was measured and it is probably due to hydrogen bonding and/or van der Waals forces between the LMW chitosan and mica. Taking the results above together, it is clear that the strong adhesion at lower pHs arises from electrostatic interaction between negatively charged mica and positively charged LMW chitosan film. The LMW chitosan film thickness measured by D_{sw} increased with an increase in pH which was confirmed by both the SFA and the tapping mode atomic force microscopy (AFM). The LMW chitosan films at higher pH bearing fewer positive charges were less likely to bind to negatively charged mica surface and consequently formed LMW chitosan aggregates on mica surfaces as observed in AFM analysis (Fig. 2).

The persistent length of the polymer, l_t, which represents the flexibility of the chain, is composed of two parts, the intrinsic part, l_p, and the electrostatic part, l_e, i.e. $l_t \simeq l_p + l_e$ (Skolnick & Fixman, 1977). At low degree of polymerization (DP), the intrinsic persistent length is linearly proportional to DP. For the LMW chitosan (DP ~ 25, and DA ~ 11%), the intrinsic persistent length is $l_p \cong 6$ nm (Rinaudo, 2006). In this range, electrostatic persistent length is comparable with the intrinsic persistent length, exhibiting about the value of $l_e \cong 4.2$ nm. The total persistent length of LMW chitosan (~10.2 nm) is similar with its contour length (~15.6 nm) at this pH, and it behaves as a rigid rod. On the highly anionic mica surface (surface charge density is about $-2.0e/nm^2$), if fully dissolved (Rojas, 2002), this multivalent rigid rod-like LMW chitosan will be compactly condensed giving rise to charge inversion (Grosberg, Nguyen, & Shklovskii, 2002). As seen from the experiment its thickness of the LMW chitosan film is thinner than higher molecular weight chitosan film (Lee, Lim, et al., 2013). The magnitude of the effective charge density can be approximated by Wigner–Seitz crystal formation, $(\sigma^*/\sigma) \simeq (\eta_1/2\pi a\sigma) \simeq 0.071$, where η_1 is the line charge density of rigid rod, a is the cylindrical radius of rigid rod, σ^* is the effect surface charge density of rigid rod, and σ is the surface charge density of rigid rod. At the end, two surfaces are oppositely charged and the electrostatic interaction between them causes attraction. The mechanism may differ for longer chain. In previous experiment, DP of high molecular weight chitosan (~150 kDa) is about 750 (Lee, Lim, et al., 2013). In such case, the contour length of chain (~343.2 nm) is much longer than persistence length, $l_c \gg l_t$. The radius of gyration is about ~41 nm ($R_g = \sqrt{l_c l_t/3}$), which is much shorter than the contour length of high Mw chitosan, i.e. we can treat the high molecular weight chitosan as Gaussian chain. Thus, if we use the same approach with short chain keeping the unit of persistence length as a single rod carrying energy of k_BT, it does not explain the difference in force between LMW chitosan film and mica. Since the valence of charge within l_t is higher for longer chain, more polymers are able to be condensed on the surface, although the effective volume charge density of chain is reduced.

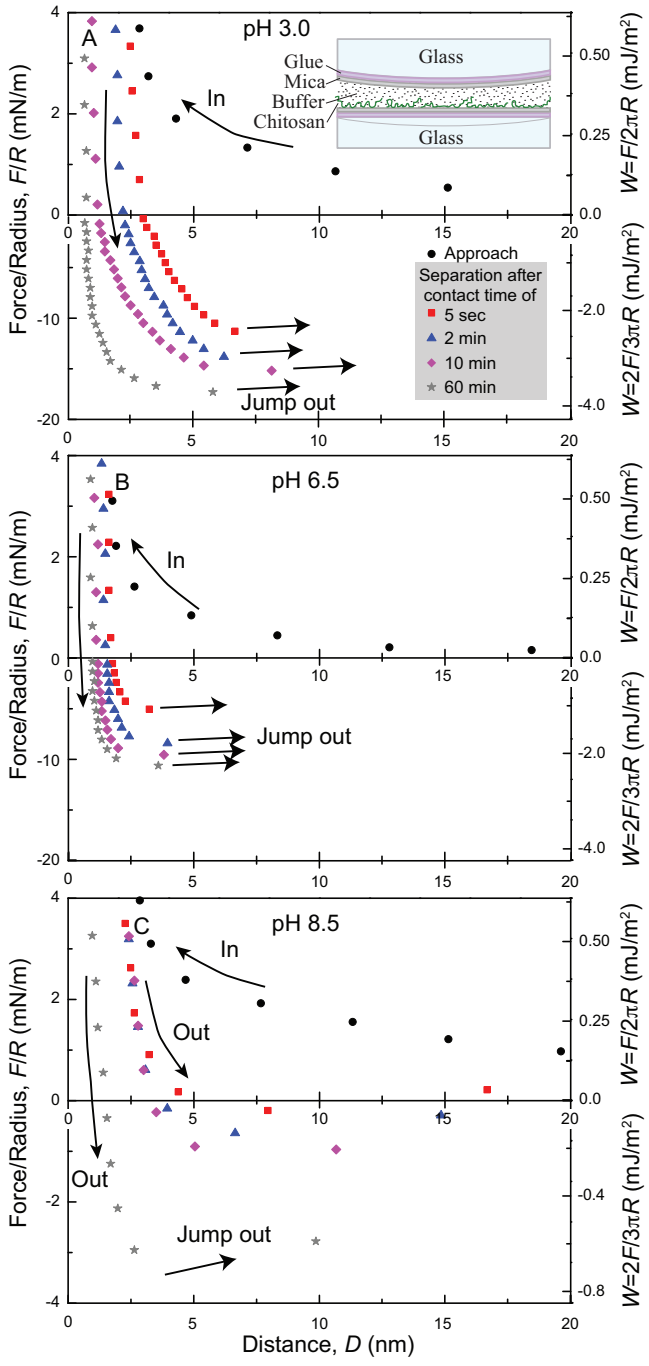

Fig. 3. Low molecular weight chitosan (LMW chitosan) adhesion to mica (asymmetric mode). Force–distance curves between low molecular weight chitosan and mica in (A) pH 3.0, (B) pH 6.5, and (C) pH 8.5. All profiles are the representative results at each pH condition.

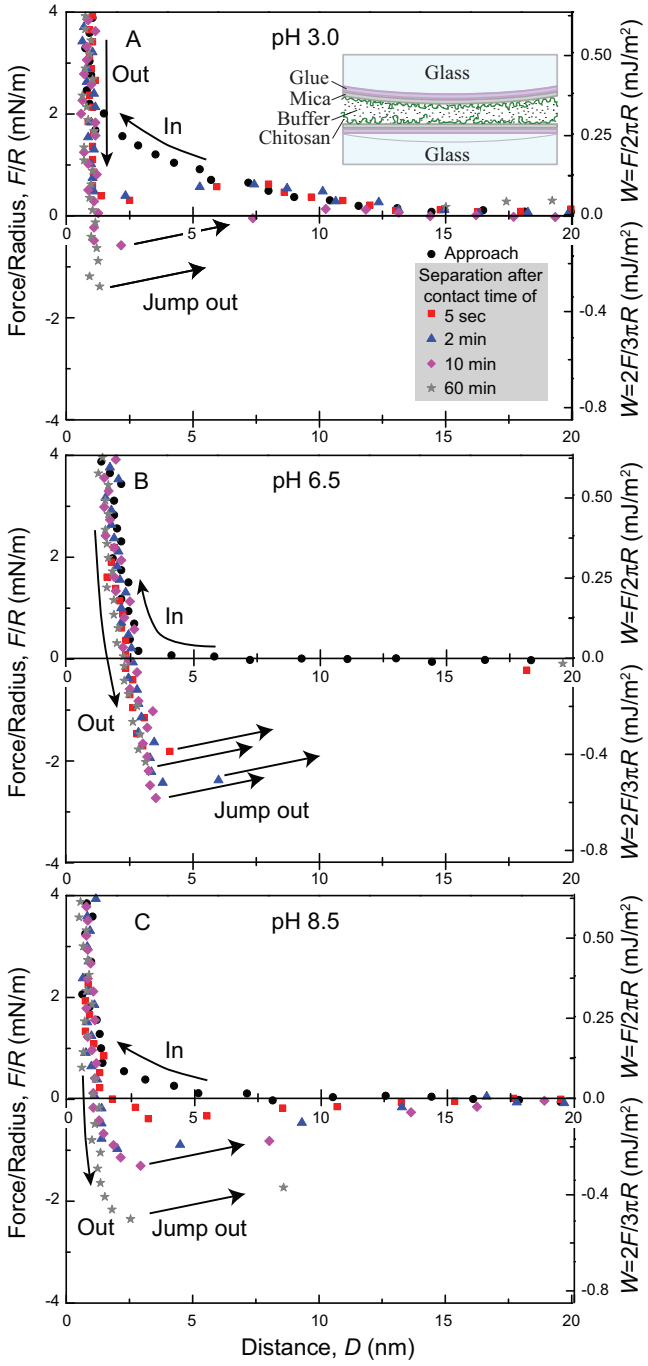

Fig. 4. Force–distance curves between two opposing low molecular weight chitosan (LMW chitosan) films in (A) pH 3.0, (B) pH 6.5, and (C) pH 8.5 (symmetric mode). All profiles are the representative results at each pH condition.

This explains thicker D_{sw} for longer chain, but stronger attraction between film and mica. As increasing pH, the line charge density of the chain is decreased. Thus, the adhesion is strongest for pH 3.0, and weakest for pH 8.5. In case of pH 6.5, perhaps the line charge density of chitosan may not be enough to induce the charge inversion, but still the oppositely charged polymers can mediate strong coupling attraction between two anionic mica surfaces.

3.2.2. Cohesion of LMW chitosan (symmetric mode)

Fig. 4 shows the force-distance profiles between LMW chitosan coated mica surfaces. The attractive force of the symmetric mode is significantly smaller than that of the asymmetric mode. Initially, when t_{ct} = 5 s, cohesion force between two opposing LMW chitosan was the largest at pH 6.5 (~1.8 mN/m) and minimum at pH 3.0 (~0 mN/m). As the t_{ct} was increased up to 1 h, cohesion force increased for all pHs. Critical contact time (t_{crit}), when cohesion force started to increase, was only observed at pH 3.0. Cohesion between the LMW chitosan films was much less than adhesion of the LMW chitosan to mica due to the electrostatic interaction. The attractive forces between the two LMW chitosan films could be largely categorized as van der Waals force, hydrophobic interactions, hydrogen bond and electrostatic force. Of these, hydrogen bonds between opposing LMW chitosan films are formed due to the

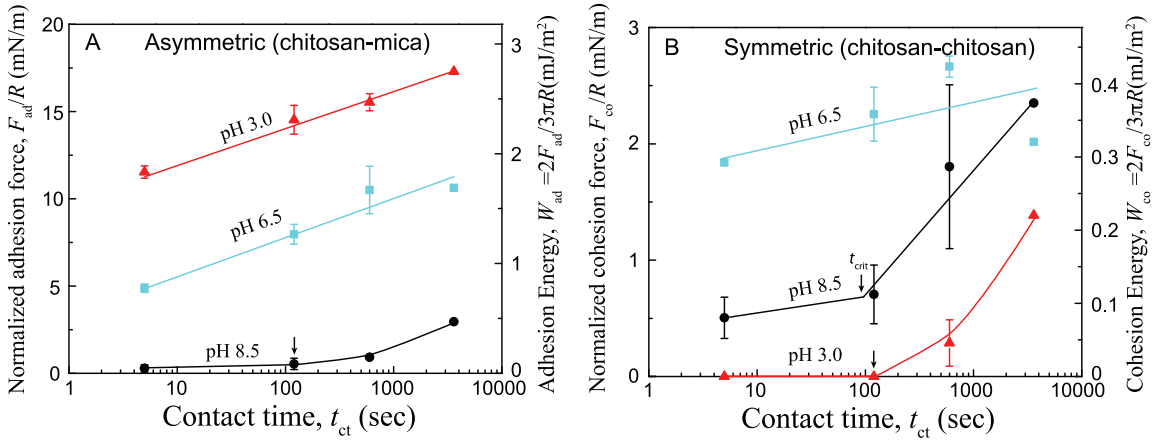

Fig. 5. (A) Low molecular weight chitosan (LMW chitosan) adhesion to mica depending on contact time and pH, and (B) Cohesion of LMW chitosan depending on contact time and pH.

presence of amine group, hydroxyl group, and acetyl group. Participating hydrogen bonds in the LMW chitosan cohesion varies on the buffer pH. Critical contact time (t_{ct}) was required for pH 3.0 as we observed in high molecular weight chitosan cohesion (Lee, Lim, et al., 2013), which is likely due to time required to overcome strong electrostatic repulsion between fully protonated amine groups and hydrogen bonding groups to meet each other between the opposing LMW chitosan films. In contrast to previously studied cohesion of high molecular weight chitosan ($W_{co} \sim 8.5$ mJ/m^2) at pH 3.0, even after the 1 h contact time, cohesion of LMW chitosan at pH 3.0 was significantly small ($W_{co} \sim 0.22$ mJ/m^2).

At pH 3.0, due to fully protonated amine groups, two mica surfaces are over-charged to induce charge inversion. From the AFM image (Fig. 2), we learned that the LMW chitosan film coated on the mica surface is very smooth (RMS roughness ~ 0.142 nm), which excludes the possible LMW chitosan aggregate domain formation and their consequent correlated attraction (Jho, Brewster, Safran, & Pincus, 2011; Meyer, Lin, Hassenkam, Oroudjev, & Israelachvili, 2005; Perkin, Kampf, & Klein, 2006). As a result, two over-charged surfaces repel each other by the electrostatic interaction at long distance. Imposing external force to contact two coated surfaces, the hydrogen bond, which is short ranged and attractive, can be established whereas the electrostatic interaction is still repulsive. So, it takes time to connect enough number of hydrogen bonds by changing its solution secondary structure from relaxed two-fold helix to extend two-fold helix, in order to overcome the electrostatic repulsion (Lertworasirikul et al., 2003; Okuyama et al., 1997). This explains the existence of t_{crit} at pH 3.0 and when $t_{ct} < t_{crit}$, only a small fraction of the amine groups of LMW chitosan molecules may participate in hydrogen bonds.

Interestingly, strongest adhesion is observed for pH 6.5 (Figure 4B). At this pH, attraction is steadily increased starting from the short contact time, $t_{ct} = 5$ s, which indicates $t_{crit} < 5$ s. The AFM image of this buffer system presented irregular surface because of partly aggregated LMW chitosan molecules. At pH 6.5, the charge density of the LMW chitosan is reduced, and as well as the persistent length. This implies that the LMW chitosan chain weakly interacts with mica surface and not likely to form a compact structure on the mica surface as in pH 3.0. Charge inversion may be suppressed or reduced significantly, resulting in LMW chitosan aggregate formation on mica. These positive charged LMW chitosan aggregates may be correlated to mediate long range electrostatic attraction between two opposing LMW chitosan coated surfaces (Sagui & Darden, 1999; Stone, 2013), not requiring long contact time for adhesion. Hydrogen bond is also easier to be formed while two surfaces are in contact. Thus, about ~0.4 mJ/m^2 appeared in initial contact time is supposed to be mainly electrostatic bonding. This interaction can be comparable to ~1.1 mJ/m^2 that of initial interaction at asymmetric case. After the LMW chitosan films are in contact, the attraction gradually increases by the formation of new hydrogen bond as the contact time increase.

At the pH 8.5 (Fig. 4C), LMW chitosan is mostly neutral due to the deprotonation of most amine groups. It may be considered as van der Waals interaction which contributes to the attraction before the t_{crit}. After t_{crit}, hydrogen bonds start to be formed. The cohesion increase after t_{crit} is about ~0.4 mJ/m^2 at pH 8.5 which is bigger than the cohesion increase (~0.1 mJ/m^2) at pH 6.5. It means that number of molecular groups and/or molecules which participate in hydrogen bonding at the pH 6.5 are less than pH 8.5.

3.3. *Molecular weight effects upon the chitosan interaction and solubility*

The adhesion of LMW chitosan (~5 kDa) to mica, mediated by electrostatic interaction, were ~40% less than that of previous studied higher molecular weight chitosan (~150 kDa) to mica (Lee, Lim, et al., 2013) whereas the cohesion of LMW chitosan coated films are reduced over 1/10 (Fig. S1). These may be attributed to the valence and flexibility of the higher molecular weight chitosan. Molecular weight effects upon adhesion and cohesion have been studied with various types of polymers (Choi, Zurawsky, & Ulman, 1999; Deruelle, Leger, & Tirrell, 1995; Jenkins, Meredith, & Wilker, 2013). Generally, increase in molecular weight induces additional chain entanglements (Choi et al., 1999). In chitosan case, participation of the hydrogen bond in chitosan may be enhanced, too. However, a more likely explanation of our results is that the persistent length of the chain is longer for the higher molecular weight chitosan, which mediates stronger electrostatic attraction with less entropic penalty. For this reason, longer chain can mediate not only stronger electrostatic interaction, but also induce more hydrogen bonds due to its flexibility. In contrast, for short chain LMW chitosan, whose contour length is shorter than persistence length, they will be very rigid, and be compactly packed on the oppositely charged surface. As a consequence, the overcharged LMW chitosan coated films in symmetric mode may repel each other, therefore it reduces the cohesion significantly, while the overcharged LMW chitosan film in asymmetric mode still shows an attraction although the magnitude is slightly smaller than high molecular weight case. At higher pH, the entropy of the chain increases which loosen the attachment of chitosan to the mica surface, and eventually, it reduces the electrostatic repulsion between chitosan molecules, and makes easier them to be aggregated seen in AFM image. The result is consistent

with long chain case. At the end, they are easier to overcome the electrostatic repulsion, and to make hydrogen bonds as increasing pH.

As stated before, main advantage of LMW chitosan over higher molecular weight chitosan is good solubility in the physiological pH range which is directly implied by our results. It has been known that the solubility has an inverse relation with cohesion energy, for example the Hildebrand solubility parameter depends on inverse square root of cohesive energy density (Barton, 1991; Hansen, 2012; Kamlet, Carr, Taft, & Abraham, 1981). Thus, the reduction of cohesion measured in LMW chitosan will lead higher solubility of LMW chitosan in physiological pH range.

4. Conclusion

We have measured the adhesion and cohesion forces of low molecular weight chitosan (LMW chitosan, 5 kDa) at different pHs and contact times, and compared results with high molecular weight chitosan (~150 kDa) which has about ~30 times longer chain length. When fully protonated, LMW chitosan is very stiff rod-like cationic chain. Two opposing LMW chitosan films are well separated due to the strong electrostatic repulsion in long distance. It requires huge external force to overcome the repulsion, which significantly reduces the cohesion of LMW chitosan. After the LMW chitosan films are brought into contact, it requires a long time to establish hydrogen bond network between two opposing surfaces. The weaker cohesion compared to the higher molecular weight chitosan explains the good solubility of LMW chitosan within physiological pH range. The contour length of the high molecular weight chitosan is much longer than that of the persistence length which results in the easier formation of the hydrogen bonds and higher possibility of the chain entanglement. Thus, longer chain can have stronger cohesion with shorter critical contact time, which reduces the solubility of high molecular weight chitosan. Contact time- and pH-dependent interaction of LMW chitosan help to accelerate its future application.

Acknowledgements

This work was supported by the Marine Biomaterials Research Center under Marine Biotechnology Program, Ministry of Oceans and Fisheries Affairs, Korea, and US Department of Energy, Office of Basic Energy Sciences, Division of Materials Sciences under Award DE-FG02-87ER-45331 (J.N.I. for the instrument modification of the Surface Forces Apparatus for the adhesion measurements and D.W.L. for the adhesion measurements). We also acknowledge the National Research Foundation of Korea Grant funded by the Ministry of Science, ICT and Future Planning (MSIP) (NRF-C1ABA001-2011-0029960 & NRF-2014R1A2A2A01006724).

Appendix A. Supplementary data

Supplementary data associated with this article can be found, in the online version, at http://dx.doi.org/10.1016/j.carbpol.2014.10.033.

References

Afshar-Rad, T., Bailey, A., Luckham, P., Macnaughtan, W., & Chapman, D. (1987). Forces between poly-L-lysine of molecular weight range 4,000–75,000 adsorbed on mica surfaces. *Colloids and surfaces*, *25*(2), 263–277.

Barton, A. F. (1991). *CRC handbook of solubility parameters and other cohesion parameters*. USA: CRC Press, LLC.

Busilacchi, A., Gigante, A., Mattioli-Belmonte, M., Manzotti, S., & Muzzarelli, R. A. (2013). Chitosan stabilizes platelet growth factors and modulates stem cell differentiation toward tissue regeneration. *Carbohydrate Polymers*, *98*(1), 665–676.

Cabrera, J.-C., Boland, A., Cambier, P., Frettinger, P., & Van Cutsem, P. (2010). Chitosan oligosaccharides modulate the supramolecular conformation and the biological activity of oligogalacturonides in Arabidopsis. *Glycobiology*, *20*(6), 775–786.

Chang, K. L. B., Tsai, G., Lee, J., & Fu, W.-R. (1997). Heterogeneous *N*-deacetylation of chitin in alkaline solution. *Carbohydrate Research*, *303*(3), 327–332.

Chatelet, C., Damour, O., & Domard, A. (2001). Influence of the degree of acetylation on some biological properties of chitosan films. *Biomaterials*, *22*(3), 261–268.

Choi, G. Y., Zurawsky, W., & Ulman, A. (1999). Molecular weight effects in adhesion. *Langmuir*, *15*(24), 8447–8450.

de Alvarenga, E. S., Pereira de Oliveira, C., & Roberto Bellato, C. (2010). An approach to understanding the deacetylation degree of chitosan. *Carbohydrate Polymers*, *80*(4), 1155–1160.

Deruelle, M., Leger, L., & Tirrell, M. (1995). Adhesion at the solid–elastomer interface: Influence of the interfacial chains. *Macromolecules*, *28*(22), 7419–7428.

Felt, O., Buri, P., & Gurny, R. (1998). Chitosan: A unique polysaccharide for drug delivery. *Drug Development and Industrial Pharmacy*, *24*(11), 979–993.

Freier, T., Koh, H. S., Kazazian, K., & Shoichet, M. S. (2005). Controlling cell adhesion and degradation of chitosan films by *N*-acetylation. *Biomaterials*, *26*(29), 5872–5878.

Grosberg, A. Y., Nguyen, T., & Shklovskii, B. (2002). Colloquium: The physics of charge inversion in chemical and biological systems. *Reviews of modern physics*, *74*(2), 329.

Hansen, C. M. (2012). *Hansen solubility parameters: A user's handbook*. USA: CRC press.

Hirai, A., Odani, H., & Nakajima, A. (1991). Determination of degree of deacetylation of chitosan by 1H NMR spectroscopy. *Polymer Bulletin*, *26*(1), 87–94.

Hirano, S., Seino, H., Akiyama, Y., & Nonaka, I. (1990). Chitosan: A biocompatible material for oral and intravenous administrations. In *Progress in biomedical polymers*. US: Springer.

Hwang, D. S., Zeng, H., Lu, Q., Israelachvili, J., & Waite, J. H. (2012). Adhesion mechanism in a DOPA-deficient foot protein from green mussels. *Soft matter*, *8*(20), 5640–5648.

Hwang, D. S., Zeng, H., Masic, A., Harrington, M. J., Israelachvili, J. N., & Waite, J. H. (2010). Protein-and metal-dependent interactions of a prominent protein in mussel adhesive plaques. *Journal of biological chemistry*, *285*(33), 25850–25858.

Ifuku, S., Nogi, M., Abe, K., Yoshioka, M., Morimoto, M., Saimoto, H., et al. (2009). Preparation of chitin nanofibers with a uniform width as α-chitin from crab shells. *Biomacromolecules*, *10*(6), 1584–1588.

Israelachvili, J. (1973). Thin film studies using multiple-beam interferometry. *Journal of Colloid and Interface Science*, *44*(2), 259–272.

Israelachvili, J., Min, Y., Akbulut, M., Alig, A., Carver, G., Greene, W., et al. (2010). Recent advances in the surface forces apparatus (SFA) technique. *Reports on Progress in Physics*, *73*(3), 16.

Israelachvili, J., & Tabor, D. (1972). The measurement of van der Waals dispersion forces in the range 1.5 to 130 nm. *Proceedings of the Royal Society of London. A. Mathematical and Physical Sciences*, *331*(1584), 19–38.

Israelachvili, J. N. (2011). *Intermolecular and surface forces: Revised* (3rd ed.). USA: Academic press, Inc.

Jenkins, C. L., Meredith, H. J., & Wilker, J. J. (2013). Molecular weight effects upon the adhesive bonding of a mussel mimetic polymer. *ACS applied materials & interfaces*, *5*(11), 5091–5096.

Jho, Y., Brewster, R., Safran, S., & Pincus, P. (2011). Long-range interaction between heterogeneously charged membranes. *Langmuir*, *27*(8), 4439–4446.

Johnson, K., Kendall, K., & Roberts, A. (1971). Surface energy and the contact of elastic solids. *Proceedings of the Royal Society of London. A. Mathematical and Physical Sciences*, *324*(1558), 301–313.

Kamlet, M. J., Carr, P. W., Taft, R., & Abraham, M. H. (1981). Linear solvation energy relationships. 13. Relationship between the Hildebrand solubility parameter, delta. H, and the solvatochromic parameter, pi.*. *Journal of the American Chemical Society*, *103*(20), 6062–6066.

Kumar, M. R., Muzzarelli, R. A., Muzzarelli, C., Sashiwa, H., & Domb, A. (2004). Chitosan chemistry and pharmaceutical perspectives. *Chemical reviews*, *104*(12), 6017–6084.

Kurita, K. (1998). Chemistry and application of chitin and chitosan. *Polymer Degradation and Stability*, *59*(1–3), 117–120.

Kurita, K. (2006). Chitin and chitosan: Functional biopolymers from marine crustaceans. *Marine Biotechnology*, *8*(3), 203–226.

Lee, D. W., Banquy, X., & Israelachvili, J. N. (2013). Stick–slip friction and wear of articular joints. *Proceedings of the National Academy of Sciences*, *110*(7), E567–E574.

Lee, D. W., Banquy, X., Kristiansen, K., Kaufman, Y., Boggs, J. M., & Israelachvili, J. N. (2014). Lipid domains control myelin basic protein adsorption and membrane interactions between model myelin lipid bilayers. *Proceedings of the National Academy of Sciences*, *111*(8), E768–E775.

Lee, D. W., Lim, C., Israelachvili, J. N., & Hwang, D. S. (2013). Strong adhesion and cohesion of chitosan in aqueous solutions. *Langmuir*, *29*(46), 14222–14229.

Lertworasirikul, A., Tsue, S.-I., Noguchi, K., Okuyama, K., & Ogawa, K. (2003). Two different molecular conformations found in chitosan type II salts. *Carbohydrate Research*, *338*(11), 1229–1233.

Meyer, E. E., Lin, Q., Hassenkam, T., Oroudjev, E., & Israelachvili, J. N. (2005). Origin of the long-range attraction between surfactant-coated surfaces. *Proceedings of the National Academy of Sciences of the United States of America*, *102*(19), 6839–6842.

Mima, S., Miya, M., Iwamoto, R., & Yoshikawa, S. (1983). Highly deacetylated chitosan and its properties. *Journal of Applied Polymer Science*, *28*(6), 1909–1917.

Muzzarelli, R. A. (2009). Chitins and chitosans for the repair of wounded skin, nerve, cartilage and bone. *Carbohydrate Polymers*, *76*(2), 167–182.

Okuyama, K., Noguchi, K., Miyazawa, T., Yui, T., & Ogawa, K. (1997). Molecular and crystal structure of hydrated chitosan. *Macromolecules*, *30*(19), 5849–5855.

Perkin, S., Kampf, N., & Klein, J. (2006). Long-range attraction between charge-mosaic surfaces across water. *Physical review letters*, *96*(3), 038301.
Rabea, E. I., Badawy, M. E. T., Stevens, C. V., Smagghe, G., & Steurbaut, W. (2003). Chitosan as antimicrobial agent: Applications and mode of action. *Biomacromolecules*, *4*(6), 1457–1465.
Ravi Kumar, M. N. (2000). A review of chitin and chitosan applications. *Reactive and functional polymers*, *46*(1), 1–27.
Rinaudo, M. (2006). Chitin and chitosan: Properties and applications. *Progress in Polymer Science*, *31*(7), 603–632.
Rojas, O. J. (2002). Adsorption of polyelectrolytes on mica. *Encyclopedia of Surface and Colloid Science*, *1*, 517.
Sagui, C., & Darden, T. A. (1999). Molecular dynamics simulations of biomolecules: Long-range electrostatic effects. *Annual review of biophysics and biomolecular structure*, *28*(1), 155–179.
Skolnick, J., & Fixman, M. (1977). Electrostatic persistence length of a wormlike polyelectrolyte. *Macromolecules*, *10*(5), 944–948.
Stone, A. (2013). *The theory of intermolecular forces*. UK: Oxford University Press.